Variation of the Divertor
Geometry in Alcator C-Mod

B. Lipschultz, J. Goetz, I.H. Hutchinson, B. LaBombard,
G. McCracken,[1] Y. Takase, J.L. Terry, P. Bonoli,
S.N. Golovato,[2] P. O'Shea, M. Porkolab, R.L. Boivin,
F. Bombarda,[3] C.L. Fiore, D. Garnier, R.S. Granetz,
M.L. Greenwald, S.F. Horne,[4] A.E. Hubbard, J.H. Irby,
E.S. Marmar, M. May,[5] A. Mazurenko, J. Reardon,
J.E. Rice, C. Rost, J. Schachter, J.A. Snipes, P. Stek,
R.L. Watterson,[6] J. Weaver,[7] B. Welch,[7] S.M. Wolfe

October 1996

[1]presently at JET Joint Undertaking, Abingdon, UK.
[2]presently at Tokyo Electron America, Beverly, MA, USA.
[3]Associazione Euratom-ENEA sulla Fusione, Frascati, Italy.
[4]presently at ASTEX, Woburn, MA, USA.
[5]The Johns Hopkins University, Baltimore, MD, USA.
[6]presently at CPClare Corporation, Lexington, MA, USA.
[7]University of Maryland, College Park, MD, USA.

Variation of the Divertor Geometry in Alcator C-Mod

Abstract

We compare divertor characteristics of three different divertor geometries varying from a 'slot' through the standard Alcator C-Mod 'vertical-plate' to a more open 'flat-plate' configuration. Differences are primarily found in the density threshold for detachment, which is 50-80% higher for the flat-plate geometry. It is inferred that volumetric emission along a flux surface is higher in the case of vertical-plate operation leading to lower temperatures at the plate and thus detachment. Other characteristics such as impurity screening, Z_{eff} and neutral pressures are unaffected.

1. Introduction

The ability to control divertor conditions is an important factor in determining the viability of the tokamak concept. Because of the very large parallel power flows envisaged for tokamak reactors (e.g. $q_{\parallel,SOL} \leq 1.0$ GW/m^2 in ITER) techniques must be developed to dissipate these power flows before they reach the plates. At the same time, any technique controlling divertor conditions must not adversely affect the core plasma. Divertor detachment is being studied as a method of achieving these goals [e.g. 1-4].

Currently, the divertor geometry in a number of experiments is being modified to allow the normal to the wetted divertor area to be directed away from the confined plasma and the opening into the divertor from the main chamber to be narrower. These changes could lead to better neutral and impurity retention in the divertor and thus less adverse effects on the core plasma [3,5-7]. There is at present minimal experimental data to support these changes. We have explored this question by changing the equilibrium flux surfaces with fixed divertor hardware; effectively changing the divertor geometry. The plasmas used in these studies were all ohmically heated 0.8 MA plasma current, 5.3 T toroidal magnetic field and a single-null equilibrium (lower x-point). The toroidal magnetic field and current are both clockwise viewed from the top of the machine.

2. Experimental Results

Although the position of the C-Mod divertor surfaces is fixed in the vacuum vessel, the flux surface equilibria can be varied such that the separatrix strike point is located on different sections of the outer divertor plate. Different effective outer divertor configurations are produced in this manner. We concentrate on the outer divertor plate because the outer divertor leg is hotter and the equilibrium (effective divertor geometry) can be varied more easily. In figure 1 we show typical

equilibria for a) the vertical-plate (the standard C-Mod and proposed ITER configuration) with strike points on vertical section; b) 'slot' with strike points at the bottom of a slot formed by the outer divertor and the parts of the vacuum vessel; and c) 'flat-plate' with strike point above the 'vertical' regions. The names used for these equilibria are not meant to be physically accurate, but only for reference.

2.1 Detachment threshold comparison

The detachment of plasma on a particular flux surface from the outer divertor plate is detected when the ratio of electron stagnation pressure at the target to that upstream in the SOL, $2n_eT_{e,plate}/n_eT_{e,SOL} \leq 0.5$, indicating a pressure deficit. A set of Langmuir probes located at the divertor plates and upstream in the SOL are used for this assessment [8]. Figure 2 shows the typical radial extent of detachment into the common flux region from the separatrix. Each flux surface is labeled by its corresponding distance outside the separatrix at the plasma midplane (ρ in mm). For the standard vertical-plate geometry, the detachment extent is a stepwise function of $\bar{n}_e$, increasing rapidly until the divertor pressure deficit reaches the flux surfaces that intersect the juncture between the vertical and semi-horizontal sections of the outer divertor plate (herein designated the 'nose' of the outer divertor, see fig. 1). The detachment extent does not increase beyond the divertor nose even for densities 2.5 x the detachment threshold. Very large deficits in plasma pressure at the divertor surface compared to upstream in the SOL are typically found after detachment; $2n_eT_{e,plate}/n_eT_{e,SOL} \sim .01$. The values of the parallel heat flux in the SOL, $q_{\parallel,SOL}$ (at the separatrix), at the detachment onset are 50-100 MW/m^2. The differences between vertical-plate and slot operation are minimal in the onset of detachment.

The flat-plate geometry resembles the open divertor geometries of earlier tokamaks. The angle of separatrix intersection with the plates in a poloidal plane is much closer to perpendicular. The surface normal over much of the plasma-wetted region points towards the core. The effect of switching the strike points to this configuration substantially increases the density threshold for detachment, figure 2. The $\bar{n}_e$ required for flat-plate divertor detachment is increased by 50-80% above that found for equivalent core conditions (input power, plasma current, etc.) with vertical-plate operation. In addition, the pressure deficit at the plate is typically smaller ($2n_eT_{e,plate}/n_eT_{e,SOL} \sim 0.1$ compared to .01 for vertical-plate). It should be noted that the extent of detachment for the vertical-plate equilibrium shown (strike point $\sim 1/2$ way down the plate) does not extend around the divertor nose even for densities above the detachment threshold for the flat-plate.

2

2.2. Comparison of divertor plasma conditions

For all of these divertor geometries, detachment occurs when the electron temperature at the divertor surface falls below a value of ~ 5 eV. Figure 3 shows $T_{e,plate}$ for the $\rho = 2$ mm flux surface as a function of $\bar{n}_e$ for the vertical- and flat-plate geometries. At low densities the divertor characteristics obtained with the two geometries are similar but as $\bar{n}_e$ is increased they diverge, with $T_{e,plate}$ dropping most rapidly for the vertical-plate. For vertical-plate operation, as $T_{e,plate}$ reaches 5 eV, detachment proceeds quickly and $T_{e,plate}$ drops abruptly to 1-2 eV. The drop in $T_{e,plate}$ with increasing $\bar{n}_e$ for the flat-plate case remains slow compared to the vertical-plate after detachment.

There are significant differences between flat- and vertical-plate operation in the volumetric emissivity profiles obtained from an array of bolometers viewing the divertor region. The brightnesses measured with the 12 detectors available for these discharges are tomographically inverted to provide local emissivities over an array of pixels 2.5 cm square [9]. That data is smoothed to provide the contour plots in figure 4. The three plots are from a single discharge. Figure 4a exhibits the typical non-detached vertical-plate emissivity profile. There is emission along the outer divertor leg with strong emission above the inner divertor nose as well. Later in the discharge after the density is raised, the divertor is detached, figure 4b. The emissivity peak has moved inside the separatrix. The strike point was then swept up the outer divertor plate to form the flat-plate equilibrium with a detached plasma, figure 4c. The emissivity peak moves back to the inner divertor but now to the inner strike point. The divertor geometry strongly affects the location of the divertor emissivity peak with respect to both the divertor plates and the separatrix.

There are also a number of similarities in divertor characteristics for the different geometries. It has previously been observed, for vertical-plate experiments, that pressure can <u>increase</u> along a flux surface ($2n_eT_{e,plate}/n_eT_{e,SOL} > 1$) for a period just prior to detachment [10]. We have found that this is true for the flat-plate operation as well. This phenomenon was not observed during slot operation due to lack of diagnostic coverage. Vertical- and flat-plate operation also have similar characteristics with regard to Z_{eff}, impurity screening [11] and neutral pressure dependence on $\bar{n}_e$ [12]. Thus one concludes that modifying the divertor shape has little effect on neutral confinement in the divertor. However, because flat-plate divertor detachment occurs at higher densities than for the vertical-plate both the midplane and divertor pressures at detachment are correspondingly increased, figure 5.

The results shown in fig. 2 are surprising in that the extent of pressure loss at the outer divertor for vertical-plate operation is limited to below the divertor 'nose' even for densities above that required to detach the flat-plate divertor plasma. One obvious difference brought about by the geometry changes is that the parallel field line length *in the divertor* is varied. We define this

'divertor connection length', $L_{x,connect}$, to be the distance along a field line ($\rho = 2$ mm flux surface) from the separatrix intersection with the outer divertor plate (strike point) to a horizontal plane located at the x-point. In a series of discharges the strike point was moved to different locations along the outer divertor plate creating equilibria varying from slot to flat-plate. The resultant detachment onset densities are plotted vs. the divertor connection length in figure 6. The corresponding location of the outer divertor strike point is also shown for each case. The dependence of $\bar{n}_{e,detach}$ on $L_{x,connect}$ is best fitted by an exponential or cubic function, much stronger than linear. We emphasize that the strongest variation in $\bar{n}_{e,detach}$ occurs for the shortest $L_{x,connect}$.

Operation with strike point at location B, shown in fig. 6, engenders characteristics of both the vertical and flat-plate. We find that detachment <u>does</u> extend beyond the vertical section of the plate to above the nose. However, the detachment threshold is significantly lower than the flat-plate The transition from vertical-plate to flat-plate operation is continuous, not a step function.

3. Discussion
3.1 Power balance

Although it is clear from the above data that there are marked differences in the detachment threshold correlated with variations in geometry, it is not clear why. To provide a framework within which to discuss the data we write down the relationship between the plasma parameters (in the SOL and divertor) and the power flowing into the SOL, $q_{\parallel}$, based on simple 1-D fluid heat transport models [e.g. 13-15]. We assume that classical parallel electron heat transport (as opposed to convection) dominates the parallel transport. This treatment is only meant as a basis for discussion, not as a replacement for more thorough 2-D models. Assuming that radiation losses occur along a flux surface only in the region from the x-point to the plate we define f_{loss}, the fraction of parallel heat flux lost to radiation, charge-exchange and ionization of neutrals [16] by:

$$q_{\parallel,x}(1 - f_{loss}) \equiv q_{\parallel,plate} \qquad (1)$$

$q_{\parallel,x}$ and $q_{\parallel,plate}$ are the parallel power flow into the divertor region (from the SOL) and to the plate respectively. Further assuming that pressure is constant on a flux surface, one can then solve the heat transport equation for the dependence of $T_{e,plate}$ on the connection length, L, upstream and core parameters:

$$T_{plate} \propto \frac{q_{\parallel,x}^{10/7}(1 - f_{loss})^2}{L^{4/7}n_{upstream}^2} \qquad (2)$$

Equation 2 thus expresses both a relationship of $T_{e,plate}$ to SOL parameters and volumetric losses along a given flux surface. We restrict our analysis to the $\rho=2$ mm flux surface hereafter. To generalize this expression still further we note that, for Alcator C-Mod discharges, $n_{upstream} \propto \bar{n}_e$.

It is intuitive that the upstream heat flux, $q_{\parallel}$ is not dependent on the divertor geometry. However, we need to make sure this is true. $q_{\parallel}$, on the $\rho=2$ mm flux surface, has been calculated by two methods:

$$q_{\parallel,x} = \frac{2}{7}\kappa_0 \frac{T_{SOL}^{7/2}(\rho = .002)}{L} ;$$ (3)

$$q_{\parallel,x} = \frac{P_{SOL}B_{tot}}{4\pi(R_0 + a)\lambda_q B_{pol}} \exp\left(- .002/\lambda_q\right)$$ (4)

where P_{SOL} is the power flowing from the core plasma across the separatrix (= P_{IN} - $P_{Rad,main}$). λ_q is the e-folding length for $q_{\parallel}$ across flux surfaces measured with the SOL Langmuir probe. Both methods yield similar scalings. The results for the second method are shown in figure 7. The similarity of attached vertical- and flat-plate $q_{\parallel}$ confirms the independence of $q_{\parallel}$ on geometry. The detached vertical-plate data points have lower $q_{\parallel}$ values due to the shift of the peak in divertor radiation inside the separatrix after detachment (figure 4b) and the resulting drop in P_{SOL}.

On the basis of previous work and figure 3 we find that $T_{e,plate} < 5$ eV is a necessary condition for detachment onset [1,8-10,17]. From this and eq. 2 we expect that $\bar{n}_{e,detach} \propto q_{\parallel,x}^{5/7}(1 - f_{loss})L^{-2/7}$. This model is unable to explain the observed variation of detachment density threshold as an effect of connection length. The dependence on L is too weak (and $q_{\parallel}$ approximately the same). Thus a variation in f_{loss} with configuration may be responsible for the differences in detachment threshold.

3.2 Collisionality

There is another viewpoint from which to compare flat- and vertical-plate operation. The collisionality of the SOL can have an important effect on temperature gradients. Eq. 2 can be rewritten to include this:

$$\frac{(R_T^{3.5}- 1)}{R_T^{3.0}} \approx \frac{2.33 \cdot \nu_{epi}^*}{(1 - f_{rad})} .$$ (5)

$R_T = T_{e,upstream}/T_{e,plate}$ and v^*_{epi} is the dimensionless collisionality for epithermal electrons. The LHS of this equation can be approximated by $R_T^{0.5}$ for $R_T \geq 1.5$. R_T must be maximized in order to have large temperature ratios [15] and achieve detachment ($T_{e,plate} \sim 5eV$). v^*_{epi} is calculated based on the electron-electron momentum collision frequency for thermal electrons, v_{ee}, and the electron thermal velocity, $v_{th,e}$:

$$v^*_{epi} \equiv \frac{L / v_{th,e}}{17 \cdot v_{ee}} = 417 \cdot \frac{n_e(10^{20}m^{-3})L(m)}{T_e^2} \qquad (6)$$

The epithermal electrons ($v_{epi} \sim 3.7 \times v_{the}$, $v^*_{epi} \approx v^*_{the}/17$) are responsible for a large share of the parallel heat flux [18-19]. Therefore we examine the functional dependence of their collisionality on geometry. We have evaluated this collisionality upstream in the SOL at the location of the SOL probe and, as expected, find no significant differences in the scaling of collisionality with $\bar{n}_e$ between the different operating geometries, figure 8. However, detachment of flat-plate discharges occurs at significantly higher collisionality than with the vertical-plate indicating that this parameter does not solely control the detachment threshold.

Referring to equation 6 we see that even in the absence of divertor radiation (we use this loosely to include all volumetric losses such as cx and ionization of neutrals), increasing collisionality leads to increases in temperature gradients and $T_{e,plate}$ falling to 5 eV. Neutrals are needed to remove momentum and finally achieve divertor detachment. Divertor radiation, through $(1-f_{loss})$, accelerates the drop in $T_{e,plate}$. The experimental values of R_T are plotted against collisionality in figure 9. In addition, equation 6 has been solved for R_T and plotted for 2 different values of f_{loss}. The non-detached vertical-plate data lie near to the line $f_{loss} \sim 0.8$. In comparison, the flat-plate data appear to have a lower f_{loss} that decreases with increasing R_T (increasing $\bar{n}_e$). Comparison of the integral of the bolometer emissivity profile (figure 4) across the outer divertor region for flat- and vertical-plate yields no significant differences within the experimental uncertainties. Therefore, one is led to conclude that the changes in f_{loss} must be more localized on flux surfaces than the spatial resolution of the emissivity profiles resulting from the bolometer tomography permits (2.5 cm).

The inference that volumetric losses along a flux surface are affected by geometry is also consistent with the dependence of $\bar{n}_{e,detach}$ on $L_{x,connect}$ seen in figure 5. That data indicates that small changes in connection length lead to large changes in $\bar{n}_{e,detach}$ (points A-C). This raises the question of whether differences in the flux surface volume below the x-point available for radiation (which is proportional to $L_{x,connect}$) are the cause of differences in f_{loss}. From equ. 2 (with $T_e \sim 5$ eV) $\bar{n}_{e,detach} \sim (1-f_{loss}) \sim \varepsilon \times (1-L_{x,connect})$ where ε is the local emissivity. If one assumes that ε is constant on a flux surface, then the predicted dependence of $\bar{n}_{e,detach}$ on $L_{x,connect}$ should be

linear. This is not consistent with the data of figure 5. In order to fit the experimental dependence we must assume that the magnitude of $\mathcal{E}$ drops below the divertor nose. It is reasonable that $\mathcal{E}$ should not be constant on a flux surface because the cooling rate [20] for typical low-Z impurities not only has a peak (at around 10-15 eV), but T_e varies along a flux surface. The bolometer emissivity profile shown in figure 4a is consistent with this argument.

The drop in (1-f_{loss}) obtained by moving the strike point from above to below the nose is large . Further movement of the strike point down the plate leads to diminishing returns in reducing the detachment threshold. This is equivalent to saying that increasing the divertor depth beyond some value is of limited value for radiation.

3.3 Neutral effects

There is another factor which could affect the relative ease of detachment for different geometries; neutrals. The neutral atom density in the last several meters of field line length leading to the divertor plate plays an essential role in momentum removal (divertor detachment). There may be differences in this density between flat- and vertical-plate operation.

Previous analyses [12, 21-22] of the role of neutrals in momentum loss for Alcator C-Mod vertical-plate operation showed that: (1) The neutral density at the outer divertor surface, inferred from Langmuir probes and H_α measurements, continually decreased, moving from the bottom of the divertor plate to the nose and above. This is consistent with neutral pressure measurements in the private flux region and at the midplane, similar to that displayed in figure 5; (2) The neutral atom densities on the vertical sections of the outer divertor plate, and corresponding neutral pressures in the private flux region, are always more than sufficient (~ 4 mTorr through flux balance arguments) to explain the observed loss in ion-neutral momentum which is typically 4 x 10^{22} m^{-2}-sec.

Based on the work described above, the neutral density in the plasma fan for flat-plate operation will be significantly lower than for the vertical-plate geometry and may be more closely correlated with the midplane pressure. In that case, flat-plate divertor detachment may await the midplane pressure rising to ~ 4 mTorr.

Lower neutral density in the plasma fan for flat-plate operation is also consistent with the $T_{e,plate}$ data of figure 3. $T_{e,plate}$ (flat-plate) remains at ~ 5 eV for a wide range in $\bar{n}_e$. Detachment, and accompanying drop in $T_{e,plate}$ could be delayed to higher $\bar{n}_e$ and the higher neutral pressures (midplane pressures) which accompany it.

4. Summary

A comparison of the characteristics of different divertor geometries has been carried out in the Alcator C-Mod tokamak. A variety of geometries have been created by varying the placement of the outer divertor strike point at different locations. The principal difference between the different divertor geometries is in the divertor detachment threshold. The vertical-plate and slot geometries have significantly lower thresholds in $\bar{n}_e$ than the flat-plate for similar upstream conditions (e.g. $q_{\|}$, ν^*). It is inferred that this difference in density threshold is due to differences in volumetric loss profiles in the divertor primarily in the region of the outer divertor nose. When the separatrix and common flux surfaces include this region (vertical plate) the losses are higher leading to lower $T_{e,plate}$ and detachment. This result argues that vertical-plate operation is useful for lowering the detachment threshold and large divertor lengths may be of marginal advantage in this regard.

5. Acknowledgments

6. References

[1] LIPSCHULTZ, B., GOETZ, J., LABOMBARD, B.L., et al., J. Nucl. Mater. **220-222** (1995) 50.

[2] MATTHEWS, G.F., J. Nucl. Mater **220-222** (1995) 104.

[3] ALLEN, S., & the DIII-D Team, Plasma Phys. & Control. Fusion **37** (1995) A191.

[4] NEUHAUSER, J.et al., Plasma Phys. & Cont. Fusion **37** (1995) A37-51.

[5] PICK, M. et al., J. Nucl. Mater. **220-222** (1995) 595.

[6] STEIBL, B. et al 16th SOFE conference, Champaign, Ill. 1995.

[7] NAGAMI, M.et al. J. Nucl. Mater. **220-222** (1995) 3.

[8] LABOMBARD B Physics of Plasmas **2** (1995) 2242.

[9] GOETZ, J.A., KURZ, C., LABOMBARD, B.L., et al, Physics of Plasmas, **3** (1996) 1908.

[10] LABOMBARD, B.L., paper I-11 12th Plasma Surface Interactions Conference, St Raphael, France, May 1996. To be published in the J. Nucl. Mater..

[11] WANG, Y. Ph. D. thesis, 'A Study of Impurity Screening in Alcator C-Mod', Plasma Fusion Center report PFC/RR-96-6.

[12] NIEMCZEWSKI, A., " Neutral Particle Dynamics in the Alcator C-Mod Tokamak', Plasma Fusion Center report PFC/RR-95-8.

[13] HOBBS, G.D., & WESSON, J.A., UKAEA Culham rept. # CLM-R61

[14] MAHDAVI, A. et al., Phys. Rev. Let. **47** (1981) 1602.

[15] STANGEBY, P.C. & MCCRACKEN, G.M., Nucl. Fusion **30** (1990) 1225.

[16] BORASS, K. & JANESCHITZ, G. Nuclear Fusion **34** (1994) 1203.

[17] STANGEBY, P.C. Nuclear Fusion **33** (1993) 1695.

[18] CHODURA, R. 'Plasma Flow in the Sheath & Presheath of a Scrapeoff Layer' in NATO Series B:Physics **131** (1986) 99.

[19] HUTCHINSON, I.H. et al, Plasma Fusion center report PFC/RR-95-12.

[20] POST, D.E. & JENSEN, R.V., Atomic Data & Nucl. Tables **20** (1977) 397.

[21] KURZ, C., LABOMBARD, B.L., LIPSCHULTZ, B. et al.Plasma Fusion Center report PFC/JA-96-34 submitted to Plasma Phys, and Cont. Fusion.

[22] NIEMCZEWSKI, A., HUTCHINSON, I.H., LABOMBARD, B.L., et al., Plasma Fusion Center Report #PFC/JA-96-12, accepted to Nuclear Fusion.
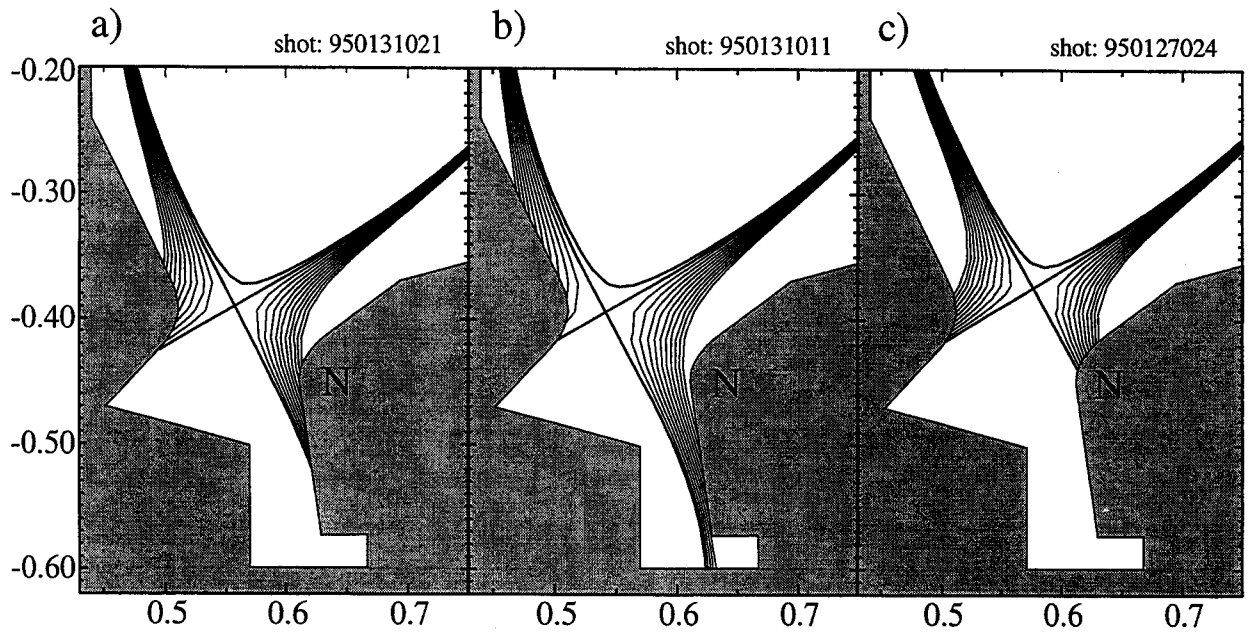
Figure 1: Typical equilibria for (a) 'vertical-plate', (b) 'slot' and (c) 'flat-plate' equilibria.. The break in slope between vertical and horizontal sections of the outer divertor plate ('nose') is indicated by an 'N'.
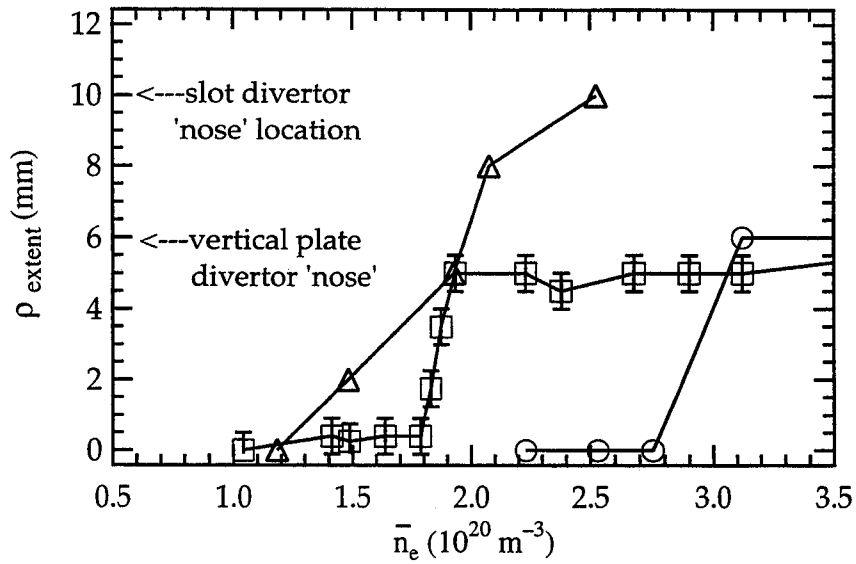
Figure 2: Extent of detachment at the outer divertor plate for 3 different divertor geometries ; □ - vertical-plate, O - flat-plate, △ - slot. ρ corresponds to the distance from the separatrix to the detachment front flux surface referenced to the midplane.
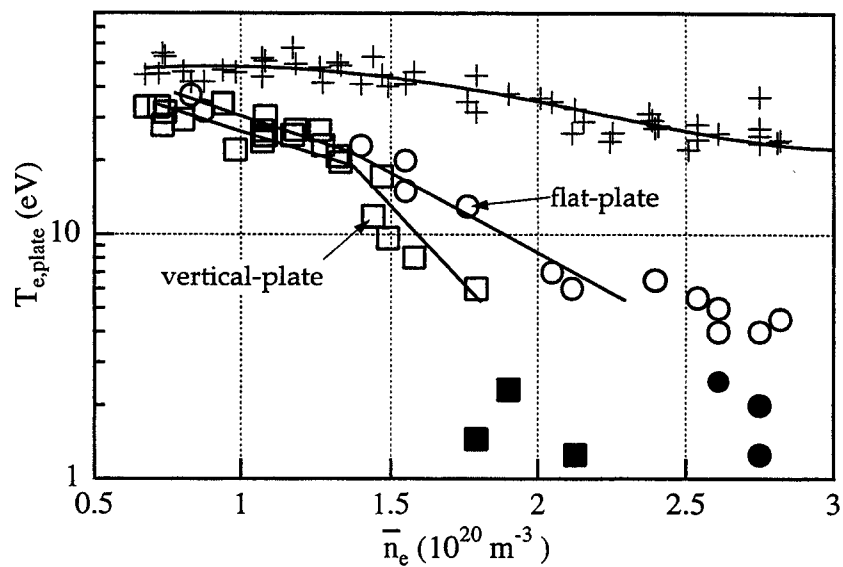
Figure 3: Divertor plate electron temperature (r = 2 mm flux surface) vs. $\bar{n}_e$. □ - vertical-plate, ○ - flat-plate, ■ & ● detached. $T_{e,SOL}$ measured by the SOL probe is shown for reference, +.
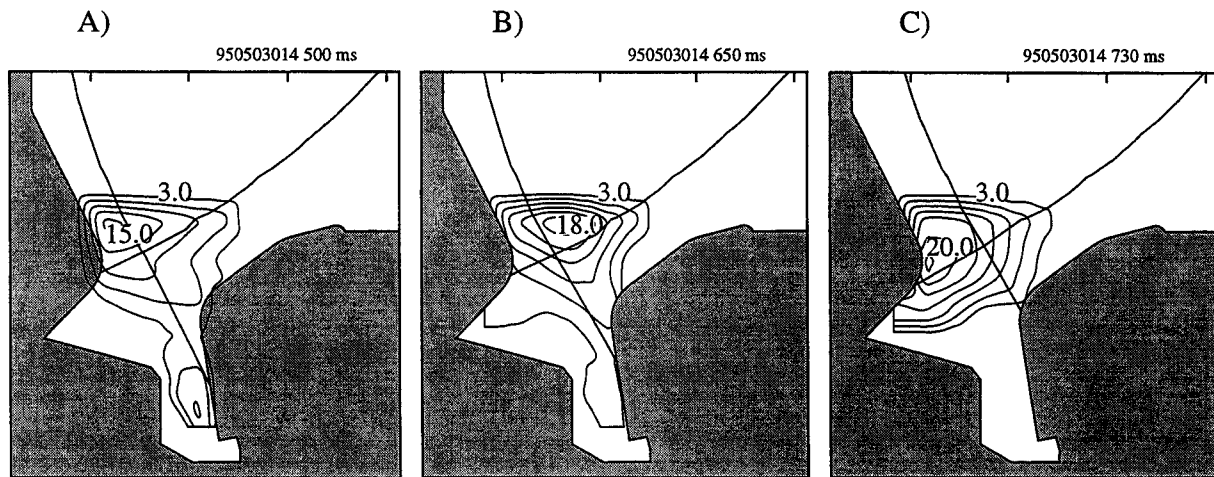
Figure 4: Volumetric emissivity profile in the divertor region for a) attached vertical-plate, b) detached vertical-plate and c) detached flat-plate operation.
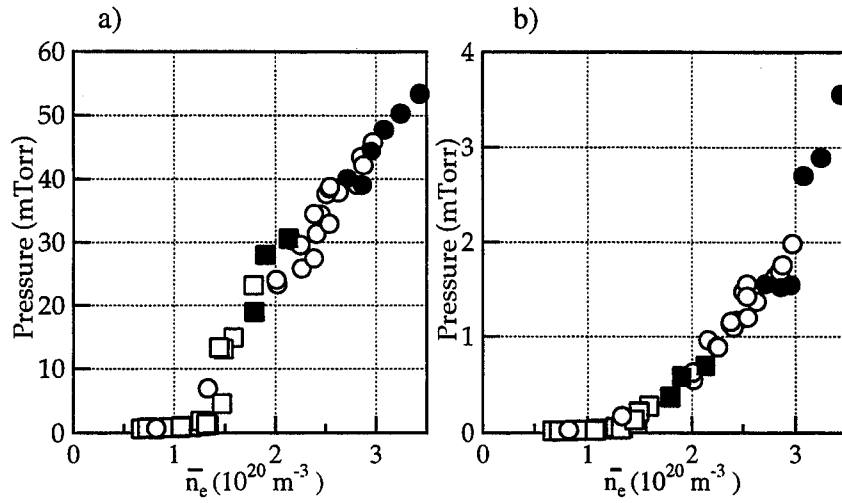
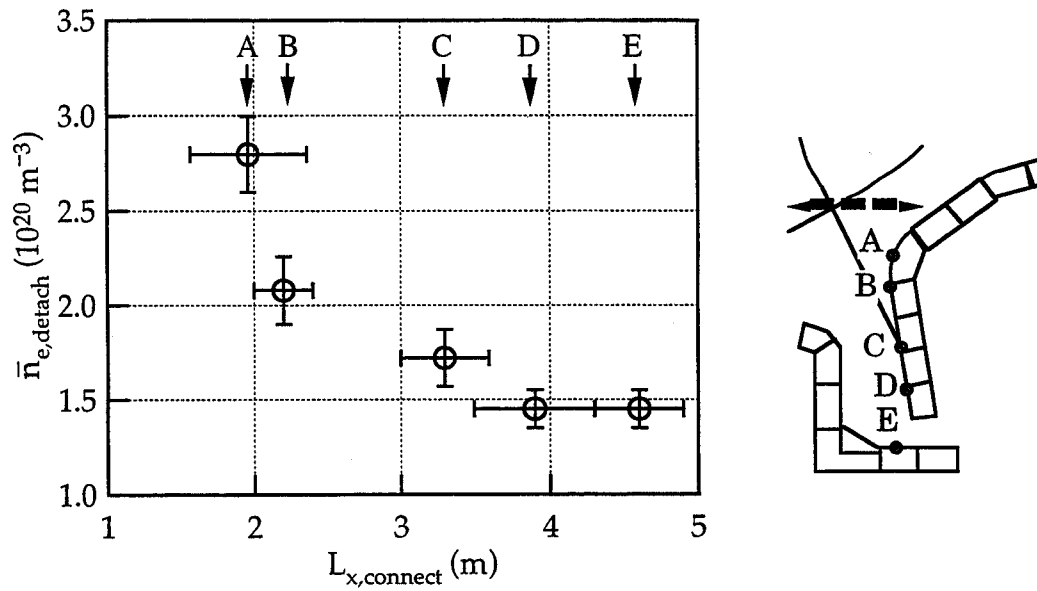Figure 5: (a) Divertor and (b) main chamber pressure vs. $\bar{n}_e$. □ - vertical-plate, ○ - flat-plate, ■ & ● detached.

Figure 6: Variation of the detachment threshold density with connection length inside the divertor ($\rho = 2$ mm). The length is measured from the horizontal plane indicated (dashed line) to the divertor plate along a field line.
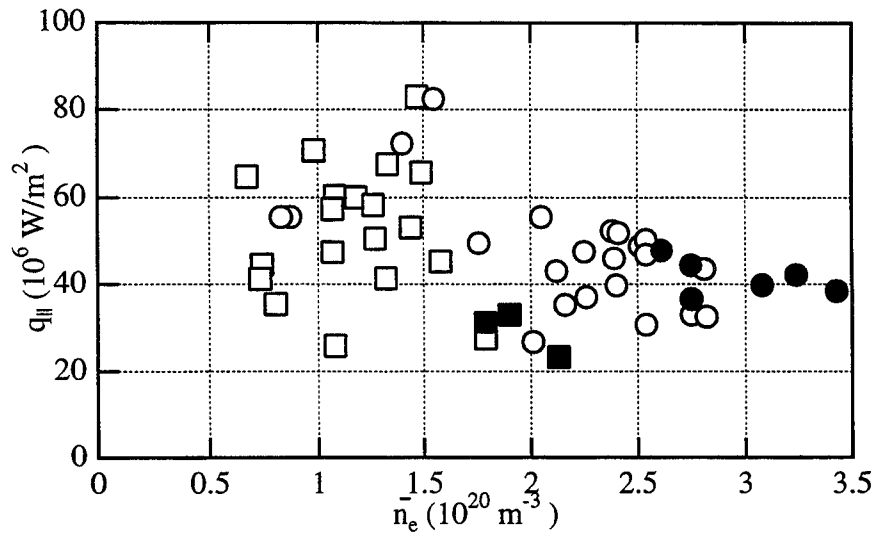
Figure 7: $q_{\parallel}$ (ρ = 2 mm flux surface) vs. $\bar{n}_e$. □ - vertical-plate, ○ - flat-plate, ■ & ● detached.
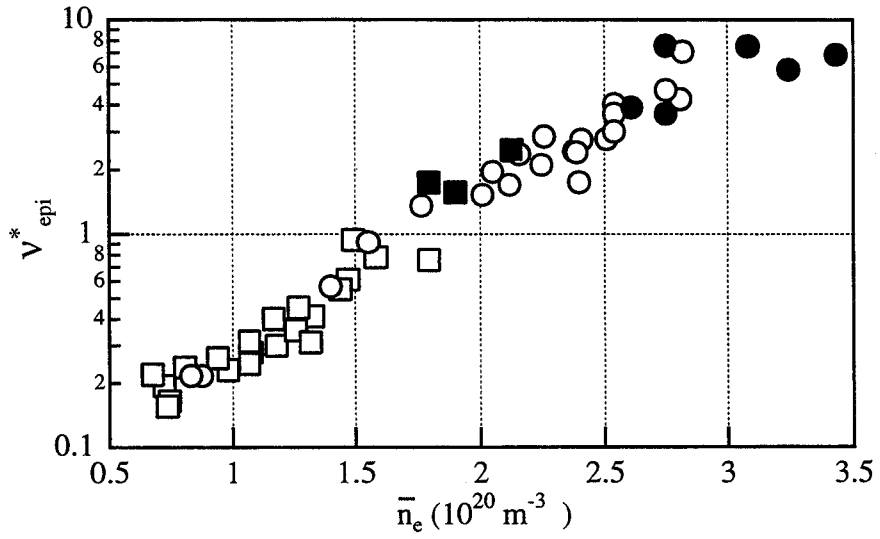
Figure 8: Upstream, SOL collisionality (ρ = 2 mm flux surface) vs. $\bar{n}_e$. $\square$ - vertical-plate, $\bigcirc$ - flat-plate, $\blacksquare$ & $\bullet$ detached.
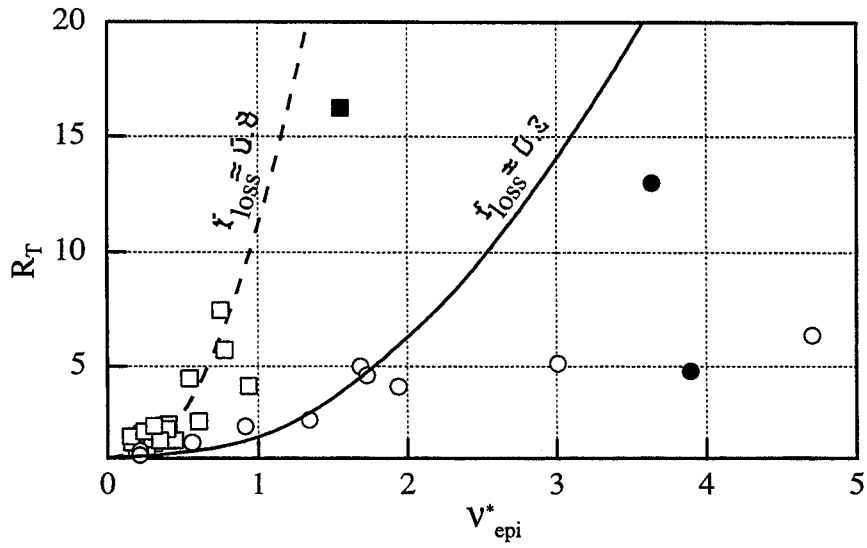
Figure 9: R_T vs. v^*_{epi} (ρ = 2 mm flux surface). □ - vertical-plate, ○ - flat-plate, ■ & ●
detached. Fits from eq. 5 are for f_{loss}= 0.2 ---- and f_{loss}=0.8 - - - -.